Advanced Technology Fuels: Materials, Experiments and Computational Modelling for SMRs and Large LWRs

Dr. Mauricio E. Cazado

Reactor Physics and Dynamic Group
Institute for Neutron Physics and Reactor Technology
Karlsruhe Institute of Technology

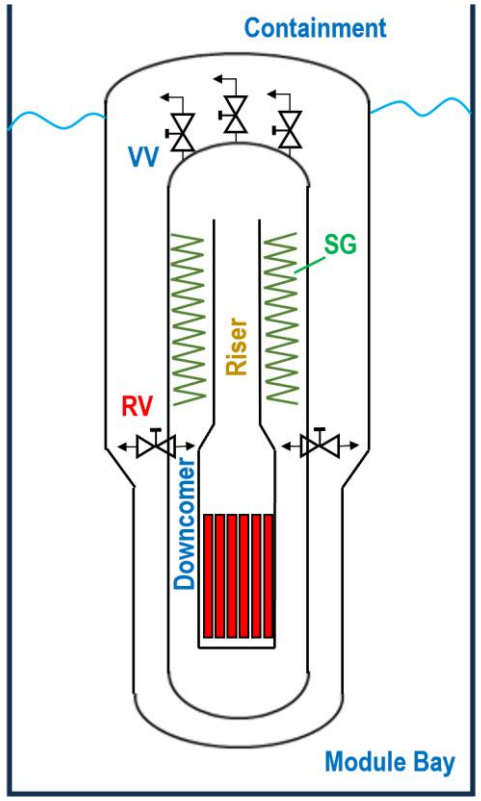

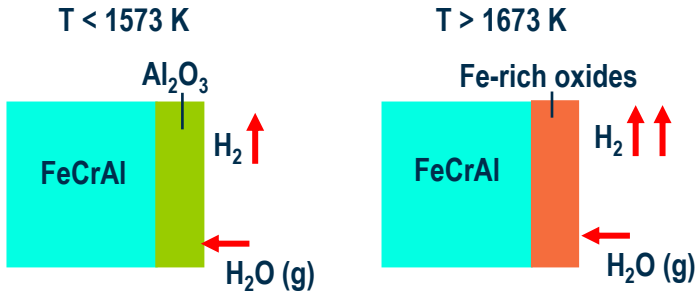

Reactor Physics and Dynamic

Content

Introduction

Requirements for Nuclear Fuels

A nuclear fuel is a safety-critical system that perform in an extreme environment

Cladding:

Serves as a first barrier against the release of FPs & enable efficient thermal transfer from the fuel to the coolant.

- Good manufacturability
- Chemical compatibility with the coolant, the fuel and assembly components.
- Corrosion resistance: LWR environments and high-temperature steam, low H embrittlement.
- Good irradiation behaviour: low thermal neutron absorption cross-section; maintain mechanical integrity, low irradiation embrittlement, etc.

Fuel Pellet:

Contains the fissile material and serves as a retention matrix for FP.

- Thermal properties: it is preferred higher melting point, thermal conductivity and lower thermal expansion coefficient.
- Mechanical properties: it is preferred higher creep rate, toughness
- Chemical properties: coolant compatibility, high FP retention and phase stability.
- Neutronic properties: high fissile density, fission cross section and low parasitic absorption are preferred.

Introduction

The Current Industry Standard

The Nuclear Industry has almost universally adopted the UO_2/Zr alloy system for LWRs.

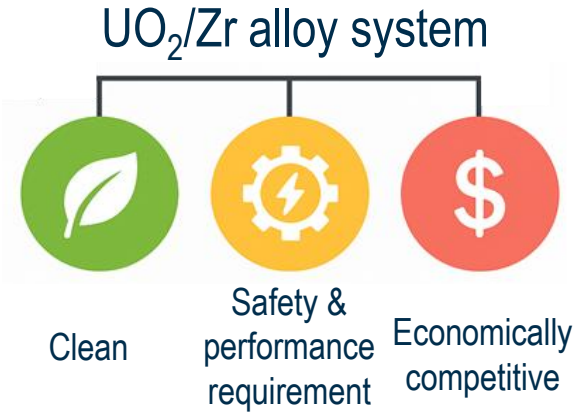

The oxide fuel-Zr alloy system has undergone decades of optimization and demonstrates **reliable performance under normal operation** and **anticipated transients**, together with **well-characterized irradiation behaviour**.

Under accident conditions (T>1200°C), Zr reacts rapidly with steam in an exothermic reaction:

$$Zr + 2H_2O(g) \rightarrow ZrO_2 + 2H_2(g) \qquad \Delta H°_r(298.15K) \approx -6.7 \text{ MJ/kg}_{Zr}$$

Under unmitigated accident conditions, this reaction can generate large amounts of hydrogen, creating an explosion risk as observed at Fukushima Daiichi.

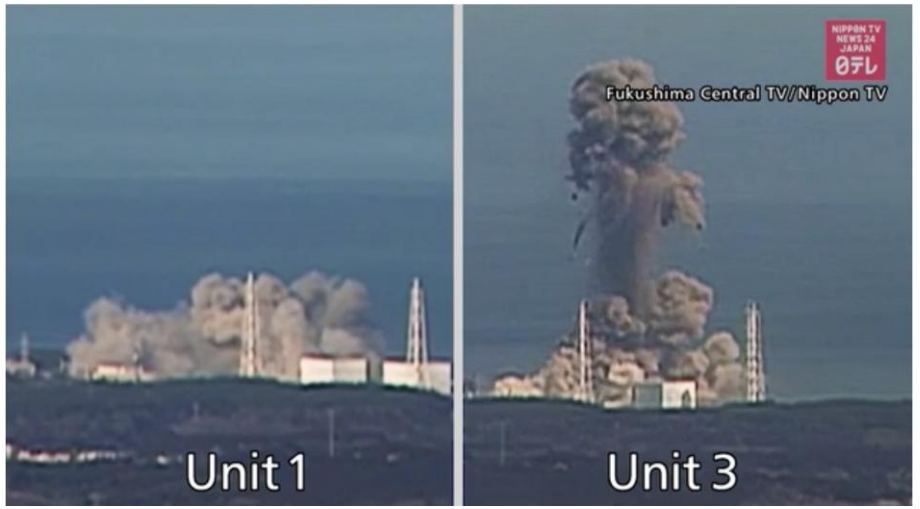

(Fairewinds Energy Education)

Introduction

Consequences of the Zr-steam reaction

$$Zr + 2H_2O(g) \rightarrow ZrO_2 + 2H_2(g) \qquad \Delta H°_r(298.15K) \approx -6.7 \text{ MJ/kg}_{Zr}$$

- **Heat Generation**: under accident conditions, the exothermic oxidation of the cladding can significantly accelerate the core degradation.
- **Hydrogen Production**: significant hydrogen generation introduces a potential explosion risk.
- **Embrittlement**: hydrogen absorption by the cladding promotes material embrittlement.

Decay heat and Zr-cladding oxidation heat: thermal power and cumulative energy during a short-term SBO (Terrani, 2018)

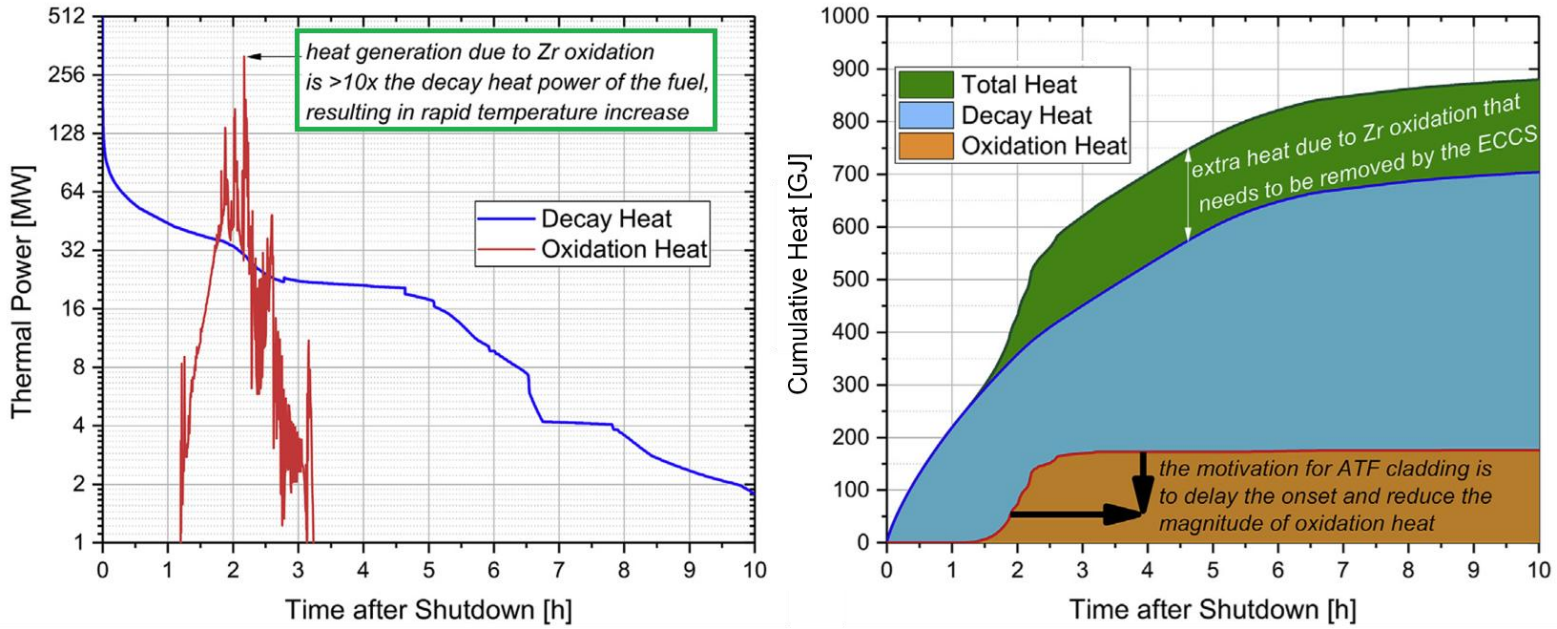

Introduction

Advanced Technology Fuels

IAEA definition: *"Enhanced accident-tolerant fuels (ATFs) are fuels that can tolerate a severe accident in the reactor core for a **longer time period** than the current UO_2 zirconium alloy fuel system, while **maintaining or improving** the fuel performance during **normal operations and operational transients**."*

Current ATF designation: Advanced Technology Fuel

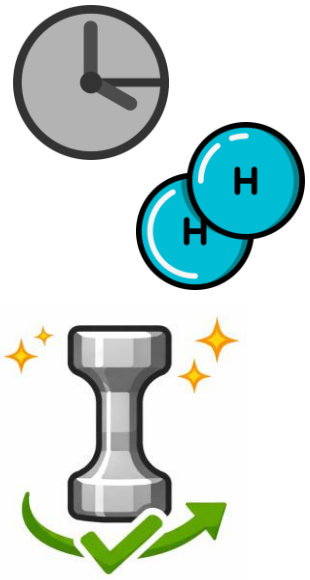

Desired characteristics

- Delay degradation and extend coping time.
- Reduced steam reaction kinetics and lower hydrogen generation rate.
- Maintaining or improving FP behaviour, thermomechanical properties

New Fuel constraints

- Backward compatibility
- Economics
- Minimal impact on the fuel cycle and on the plant operations.

Advanced Fuel and Cladding Concepts

Advanced Fuels

- Improved UO_2
  - Doped UO_2
    - Cr_2O_3 doped UO_2, Cr_2O_3-Al_2O_3 doped UO_2
    - Ceramic microcell UO_2
  - High-thermal conductivity UO_2
    - Metallic additive
      - CERMET, Mo-modified UO_2, Metallic microcell UO_2
    - Ceramic additive
      - BeO-modified UO_2, SiC/diamond modified UO_2
- High-density Fuel
  - Silicide, Nitride, Carbide, & Metal
- Encapsulated Fuel

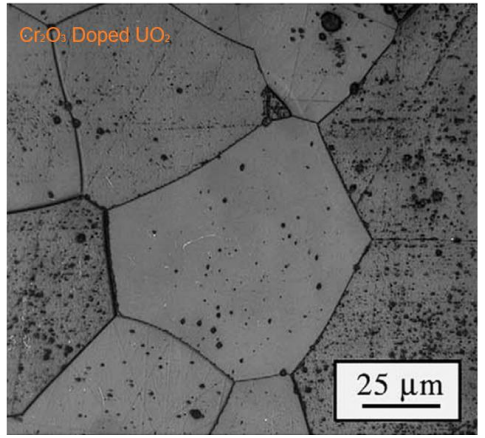

UO_2 + 0.05 wt% Cr_2O_3 (Bourgeois, 2001)

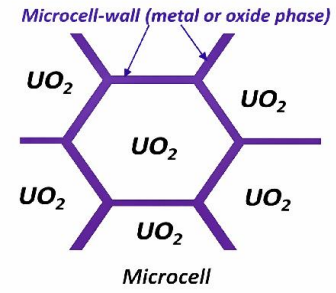

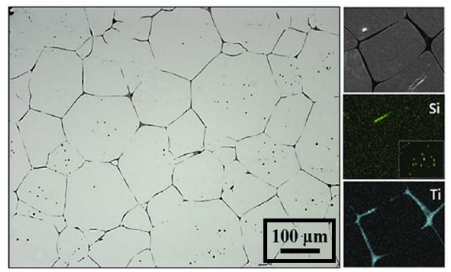

Si-Ti-O microcell UO_2 (Kim, 2018)

Advanced Fuel and Cladding Concepts

Advanced Claddings

- Coated Zr-alloys
  - Metallic coatings → Cr, Cr alloys, FeCrAl, Cr/FeCrAl
  - Ceramic coatings → Nitrides: CrN, TiN, TiAlN, CrAlN; MAX phases: Ti_2AlC, Cr_2AlC, Zr_2AlC
- Advanced Steels: FeCrAl
- Refractory Metals: Lined Mo-alloy
- SiC & SiC/SiC composites

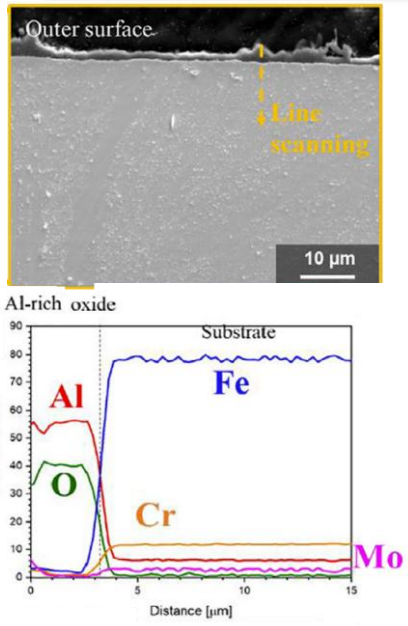

FeCrAl ox. Test (Kim, 2022)

SiC/SiC tube (Koyanagi, 2017)

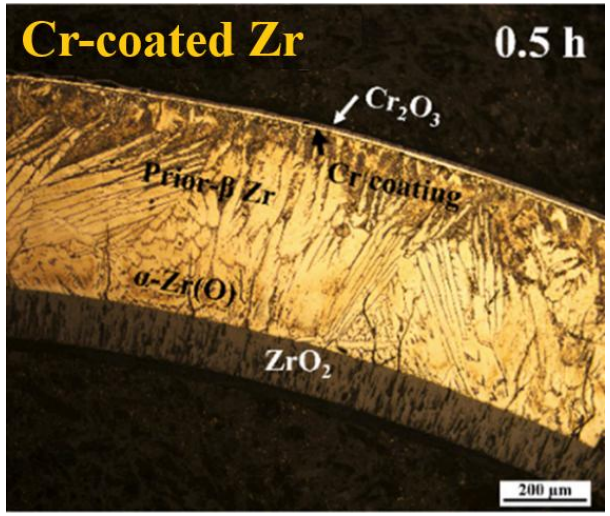

Cr-coated Zr alloy (Deng, 2023)

ATF Characteristics & Experiments

Advanced Fuels – Doped UO_2

Main desirable attributes:

- Enhancing the FPs retention;
- Minimising Pellet-Cladding Interaction.

Cr_2O_3 and Al_2O_3-Cr_2O_3 doped UO_2

- Larger grain structure: aiming at increasing the FPs retention and fuel viscoplasticity.
- Thermal behaviour: No measurable differences in heat capacity, CTE, T_m and thermal diffusivity in unirradiated fuel
- Thermo-mechanical behaviour: high-dimensional and microstructural stability up to high burnup. Negligible in-pile densification (IFA-677).
- FGR behaviour: improved intragranular fission gas retention (30% less than standard fuel)

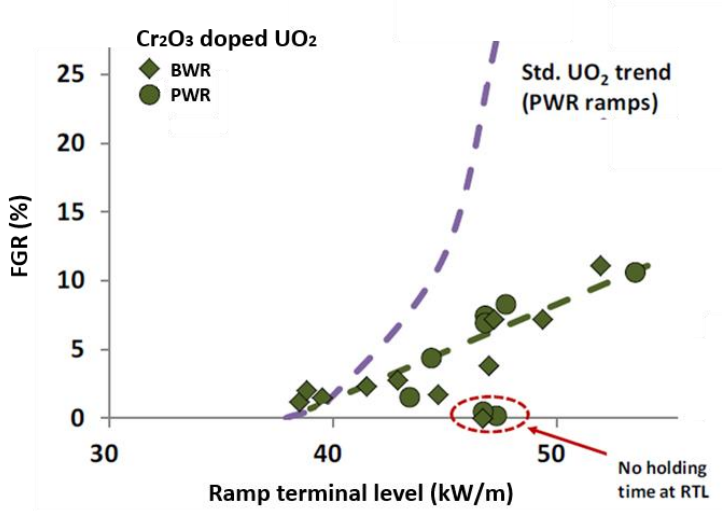

Comparison of fission gas release kinetics in UO_2 and Cr_2O_3-doped UO_2 fuels in ramp testing conditions (Delafoy, 2016)

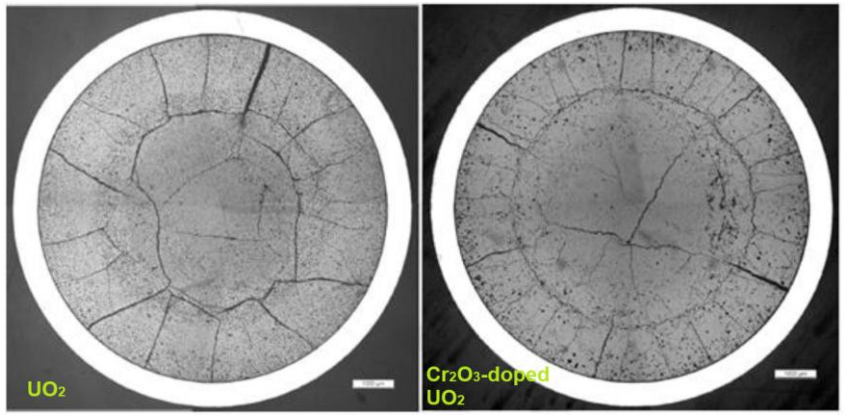

Comparison of post-ramp fuel microstructure for standard UO_2 and Cr_2O_3-doped UO_2 (Delafoy, 2016)

ATF Characteristics & Experiments

Advanced Fuels – High-thermal conductivity UO_2

Metallic additive fuel concept

- Low volume fraction (5 to 10%) of highly conductive metallic additive to increase the conductivity of the pellet.
- Additives like Mo or Cr exhibit mild neutron absorption; therefore, a slight increase in enrichment is required.
- High-thermal conductivity can provide lower fuel temperature and larger thermal safety margin during transients.
- Internal cell walls delay iodine release, thus lowering iodine-induced stress corrosion cracking (SCC/I).
- Mo is prone to high steam oxidation rate. Tests at 500°C showed that the pellets retained their structural integrity.

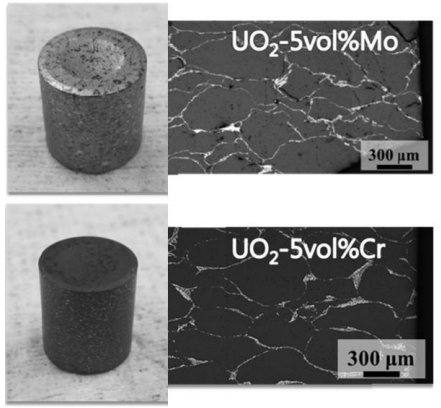

Sintered pellet and microstructures for 4.70 wt.% Mo and 3.34 wt.% Cr metallic microcell UO_2 (Kim, 2016).

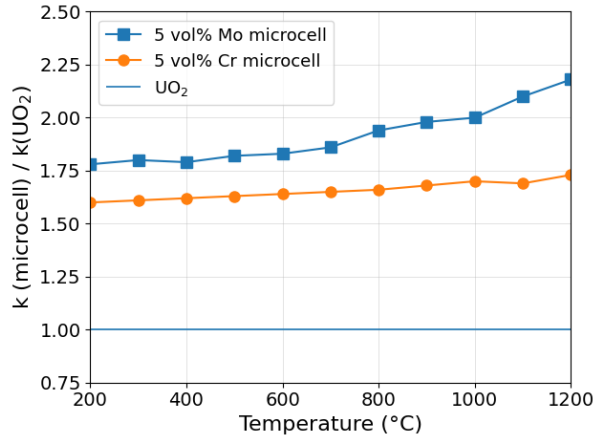

The thermal conductivity measurement results of metallic microcell UO_2 pellets (Kim, 2016)

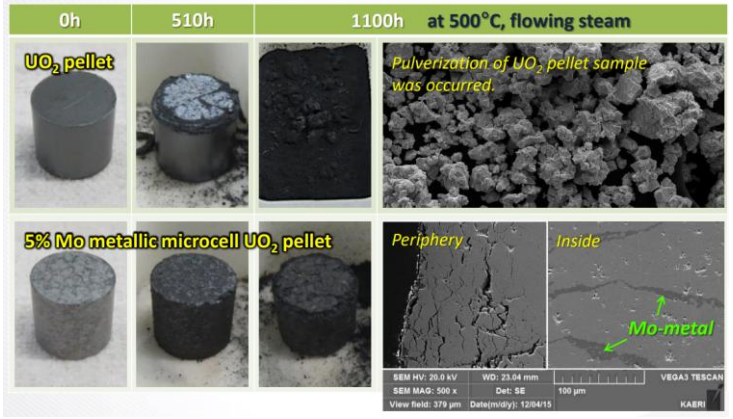

UO_2 and Mo microcell UO_2 steam oxidation test at 500°C (Kim, 2023).

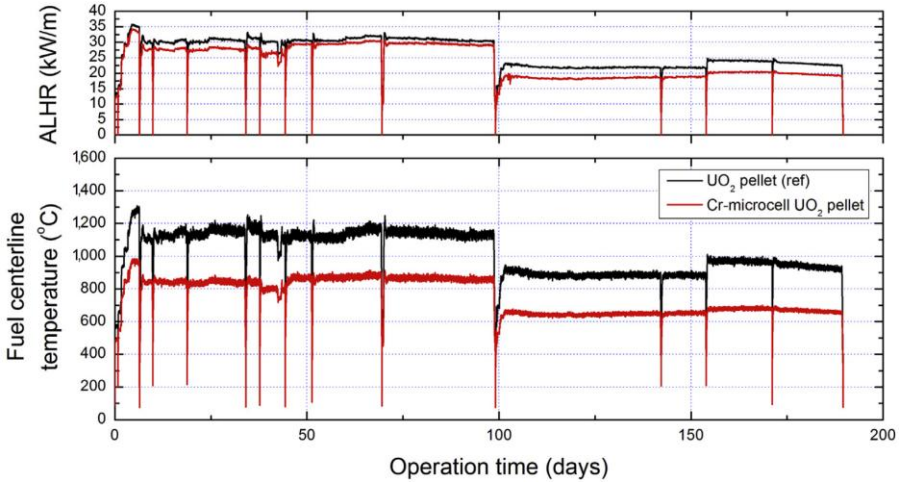

Online measurement data of fuel centerline temperature of UO_2 and Cr microcell UO_2 ALHR, averaged linear heat generation rate (Kim, 2018)

ATF Characteristics & Experiments

Advanced Cladding – Cr-coated Zr alloy

- Metallic Cr coatings deposited on Zr alloys (e.g., Zircaloy-4, M5, ZIRLO), mainly via PVD and cold-spray techniques.
- Thickness coating typically 5-30 μm: thicker coating provides larger Cr amount for oxidation protection but increase neutronic penalties and changes in mechanical properties.

Advantages

- Good compatibility with existing fuel designs
- Coating thickness < 20 μm have minimal impact on the neutron economy and can be compensated with by slight design modifications.
- High steam oxidation resistance: Protective Cr_2O_3 up to ~1600 K.
- The protective Cr_2O_3 and Cr layer act as barrier that reduce hydrogen migration to the Zr substrate, thus mitigating hydrogen embrittlement.

Disadvantages

- Eutectic formation at ~1600 K → rapid degradation of the cladding integrity.
- The protective effect of the Cr layer is lost after Cr-Zr Eutectic.
- Interdiffusion: at high temperatures, Cr diffuses into the Zr and forms a brittle intermetallic $ZrCr_2$.

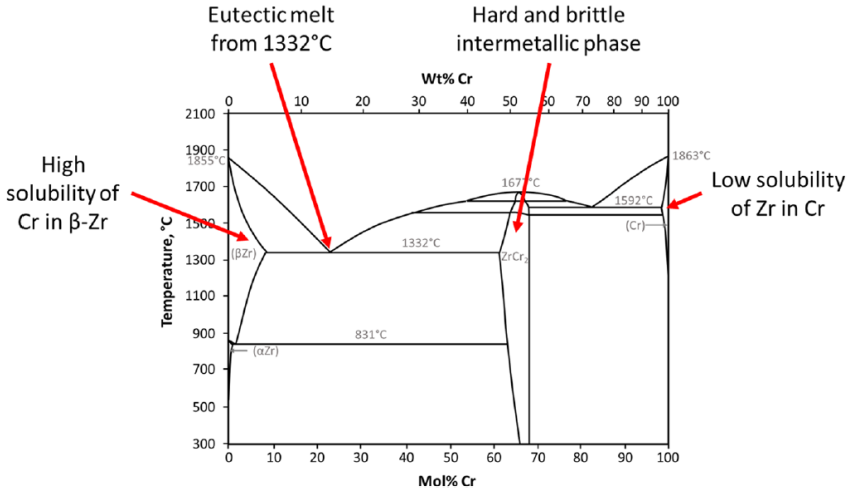

Phase diagram of Zr-Cr (Steinbrück, 2024; Arias, 1986).

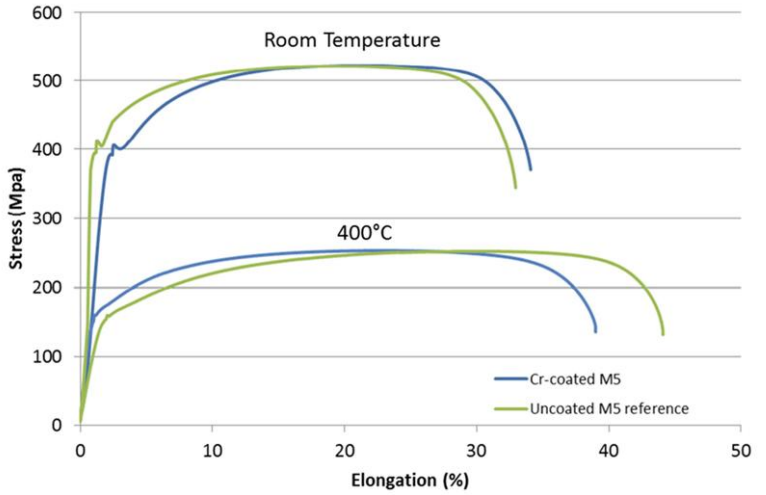

Tensile tests at room temperature and 400 °C of M5 ® and Cr-coated M5® (coating thickness < 20 um) (Bischoff, 2016).

ATF Characteristics & Experiments

Cr-coated Zr alloy: Corrosion Resistance

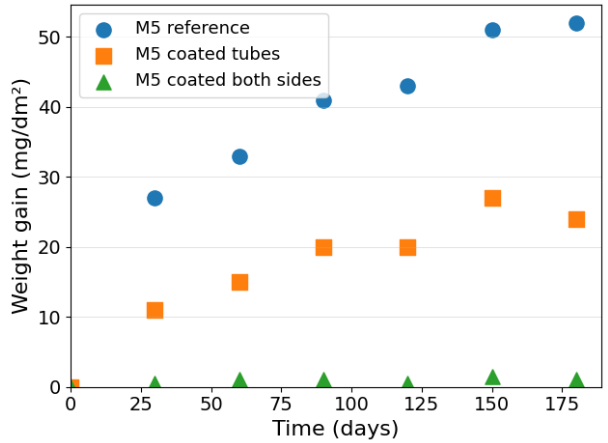

Corrosion kinetics of Cr-coated M5® exposed to PWR water at 360°C (Bischoff, 2016)

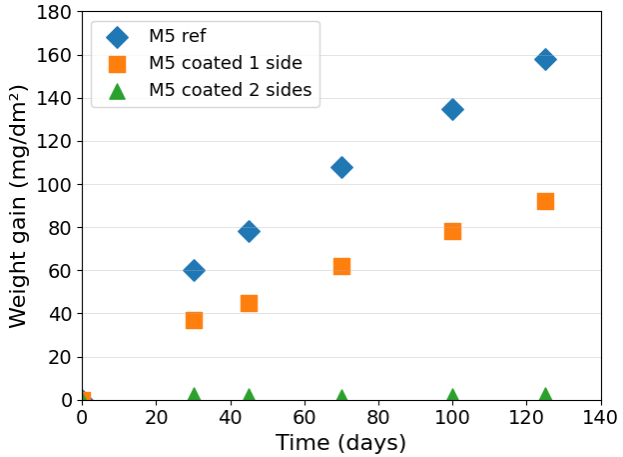

Corrosion kinetics of Cr-coated M5® exposed to steam at 415°C (Bischoff, 2016)

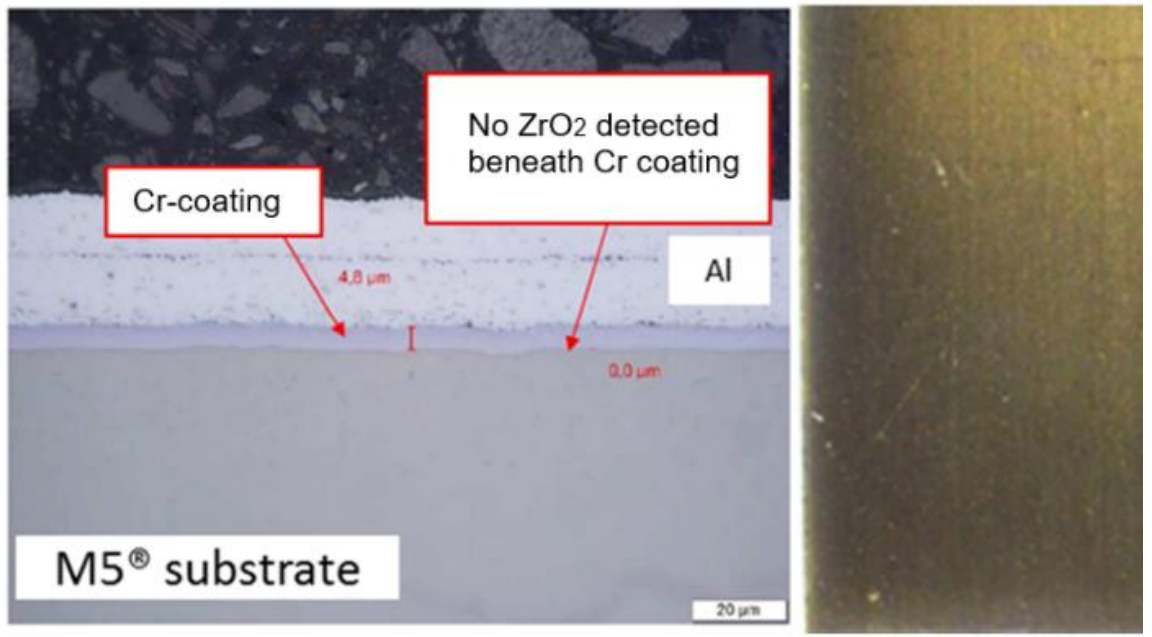

M5® Cr-coated sample after corrosion in 360°C PWR water for 30 days. Aluminum foil is used for sample preparation. Golden color suggests that chromia layer is less than 100 nm. (Bischoff, 2016)

ATF Characteristics & Experiments

Cr-coated Zr alloy: High-Temperature Steam Oxidation

- Cr-coatings are protective at the beginning of the oxidation: oxide layer is adherent

$$2Cr + 3H_2O(g) \rightarrow Cr_2O_3 + 3H_2(g)$$

- Transition between protective and non-protective coating: progressive and smooth acceleration of the weight gain evolution:
  - Inward oxygen diffusion and outward Zr intergranular diffusion in the residual metallic Cr layer.
  - Zirconia stringers nucleate and grow at the Cr grain boundaries, promoting the inwards diffusion of oxygen anions.

- Non-protective coating: oxidation of the Zr substrate

- Formation of the $ZrCr_2$ intermetallic contributes to the Cr layer consumption.

Schematic representation of the non-protective stage of Cr/Zr oxidation at HT steam (Brachet, 2020)

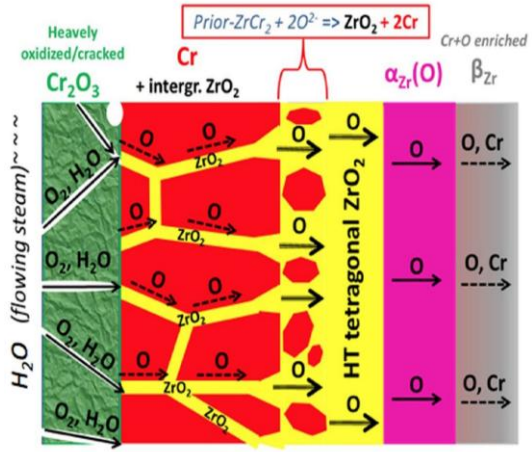

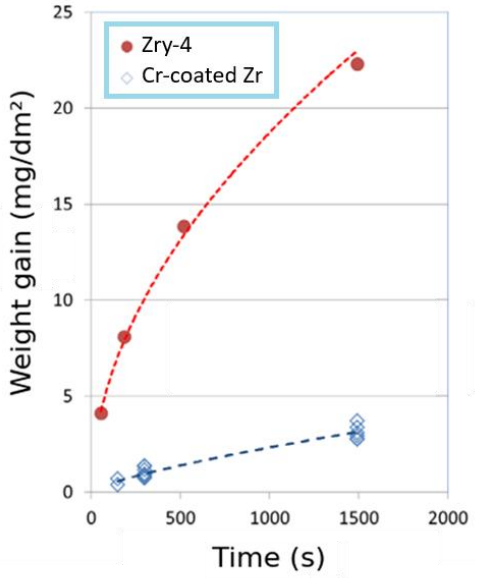

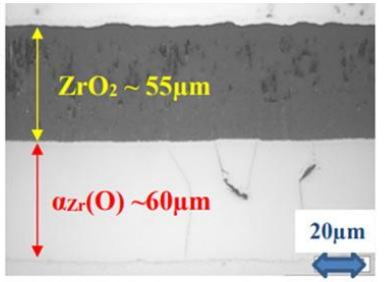

Zry-4 after 300 s of oxidation

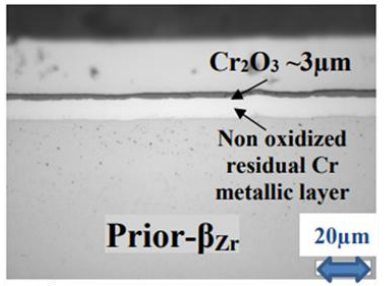

Cr-coated Zr after 300 s of oxidation

Steam oxidation behaviour comparison for Zry-4 and Cr/Zry-4 (Schuster, 2015)

ATF Characteristics & Experiments

Cr-coated Zr alloy: HT Steam Oxidation

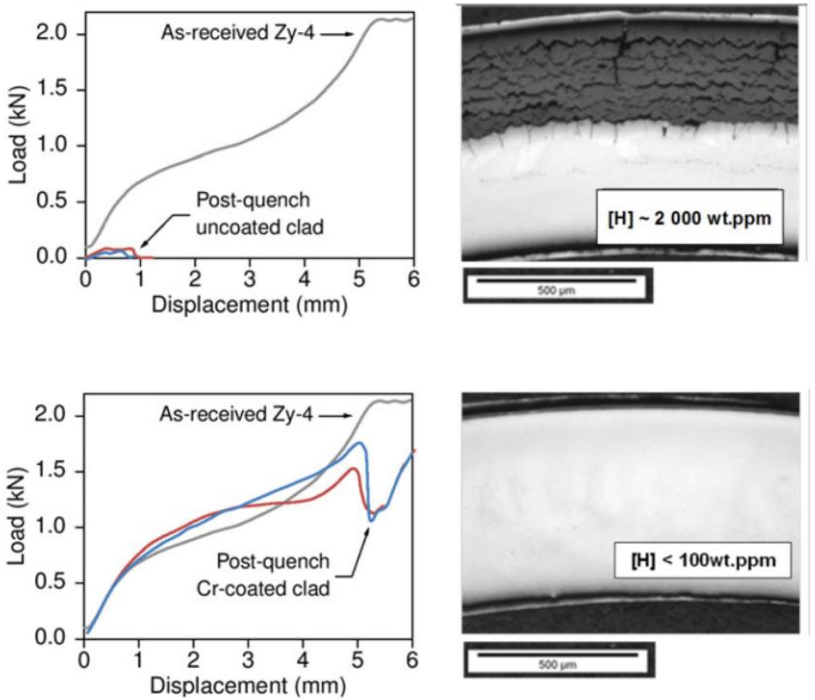

Ring compression test at 135 °C after 15000 s of HT steam oxidation at 1000°C for Zry-4 and Cr/Zry-4 samples (Schuster, 2015; IAEA, 2018).

- **Cr-coated cladding:** after 15 000 s steam oxidation at 1000 °C, retains most of its residual strength and ductility.
- **Uncoated cladding:** high hydrogen uptake → negligible residual strength and ductility.

Cr-coated Zr alloy: HT Creep behaviour

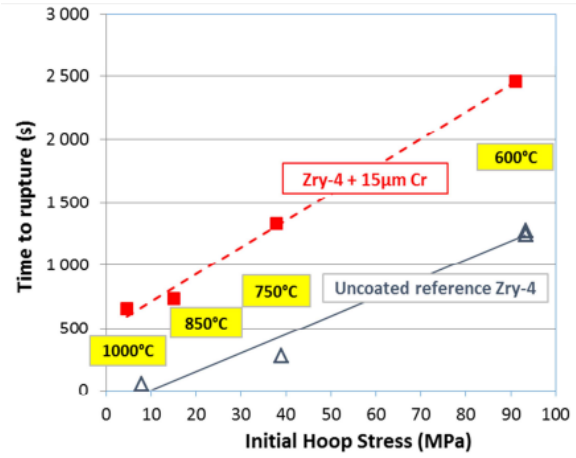

Rupture time vs the initial hoop stress of uncoated and 15µm Cr-coated Zry4 clad segments for isothermal creep tests performed at different temperatures (Brachet, 2016)

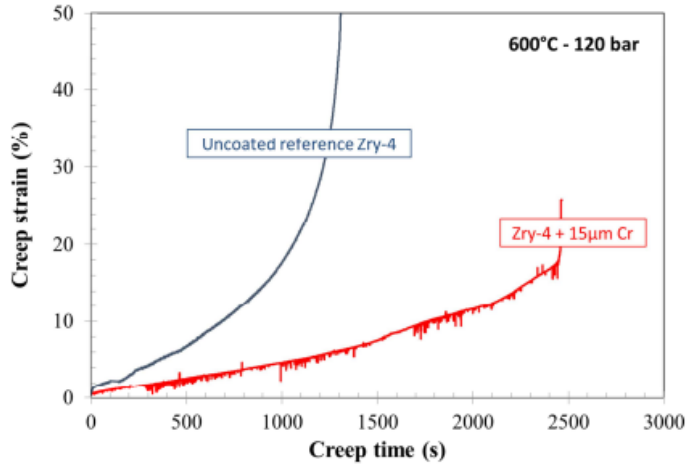

Creep curves for uncoated and 15 µm Cr-coated Zry-4 clad at 600°C and internal pressure of 120 bar (Brachet, 2016)

15 µm Cr coating provides a strengthening effect at high temperature.

ATF Characteristics & Experiments

Advanced Cladding – FeCrAl alloys

- Fe-based alloy with 12 – 24 wt% Cr and 3 – 6 wt% Al.
- Nuclear grade FeCrAl: 10 – 13 wt% Cr and 5 – 6 wt% Al. Additional additives to improve oxidation resistance and mechanical properties: Mo and Y.

Alloy /wt%	Fe	Cr	Al	Mo	Y	C	Si
B136Y3	Bal.	12.97	6.19	-	0.03	<0.01	-
C26M2	Bal.	11.87	6.22	1.98	0.03	<0.01	0.2

Advantages

- Superior oxidation resistance at high temperatures due to the formation of a protective layer of Al_2O_3: strong protection below 1300 °C.
- Superior mechanical properties when compared to Zr alloy.
- Lower hydrogen generation under steam oxidation.

Disadvantages

- Higher neutron absorption cross-section than Zircaloy: cladding thickness must be reduced.
- Tritium permeability due to lack of hydrogen isotopes trapping, but lower than pure Fe.
- Under neutron irradiation, FeCrAl with high Cr content (20-22 wt%) is susceptible to Cr-rich α' phase → irradiation embrittlement.
- Interaction between UO_2 and FeO forming an Eutectic at ~1335°C

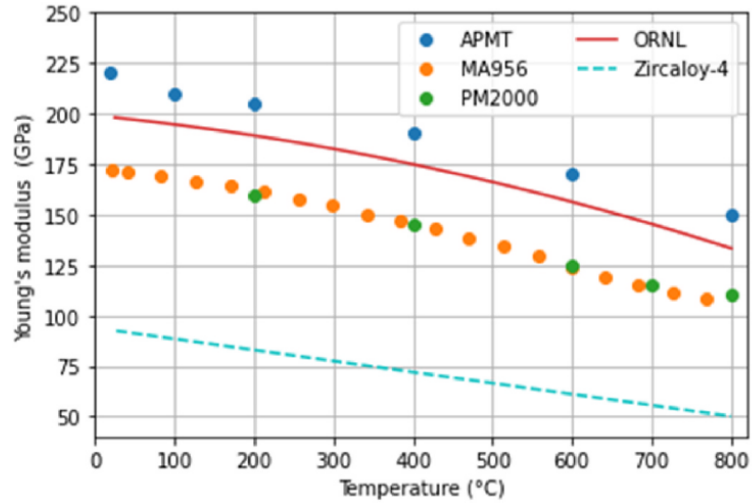

Young's modulus as a function of temperature (Aragon, 2022)

ATF Characteristics & Experiments

FeCrAl alloys: Water Corrosion

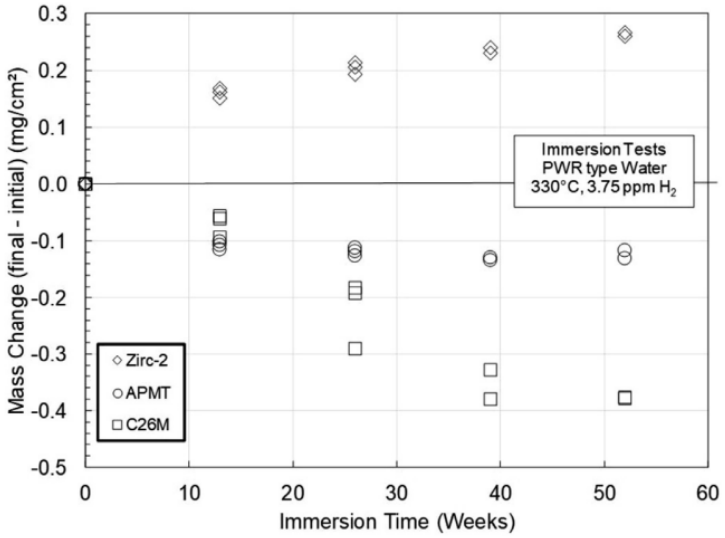

Mass change vs time for Zry-2, APMT, and C26M tube samples in simulated PWR hydrogenated water at 330°C (Yin, 2021)

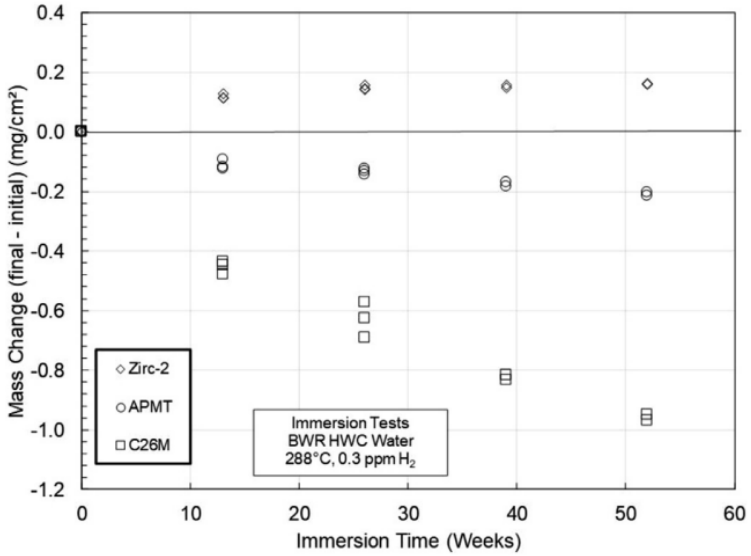

Mass change vs time for Zry-2, APMT, and C26M tube samples in simulated BWR hydrogenated water at 288°C (Yin, 2021)

- FeCrAl shows slight mass loss due to alumina dissolution (Yin, 2021).
- Cladding wall thinning remains negligible over in-reactor residence time

Alloy /wt%	Composition
Zry-2	Bal. Zr, 1.4Sn, 0.05Ni, 0.12Fe, 0.1Cr
APMT	Bal. Fe, 21Cr, 5Al, 3Mo, Y, Zr, Ti.
C26M	Bal. Fe, 12Cr, 6Al, 2Mo, 0.05Y

ATF Characteristics & Experiments

FeCrAl alloys – HT Steam oxidation

- Alloys under study with variable composition affecting the overall behavior with impact in the oxidation processes.
- Kim et al. (2022) studied isothermal and transient steam oxidation ranging temperatures between 500°C and 1500°C.

Oxidation behavior changes dramatically between 1300°C and 1400°C: Eutectic point in the Fe-O system at ~1370°C.

≤1300°C: Aluminum oxidation

>1400°C: Iron oxidation dominates the reaction

	As-received	After isothermal oxidation test (20 hours)									
		600°C	700°C	800°C	900°C	1000°C	1100°C	1200°C	1300°C	1400°C	1500°C
B136Y3											
C26M2											

(Kim, 2022)

Alloy /wt%	Fe	Cr	Al	Mo	Y	C	Si
B136Y3	Bal.	12.97	6.19	-	0.03	<0.01	-
C26M2	Bal.	11.87	6.22	1.98	0.03	<0.01	0.2

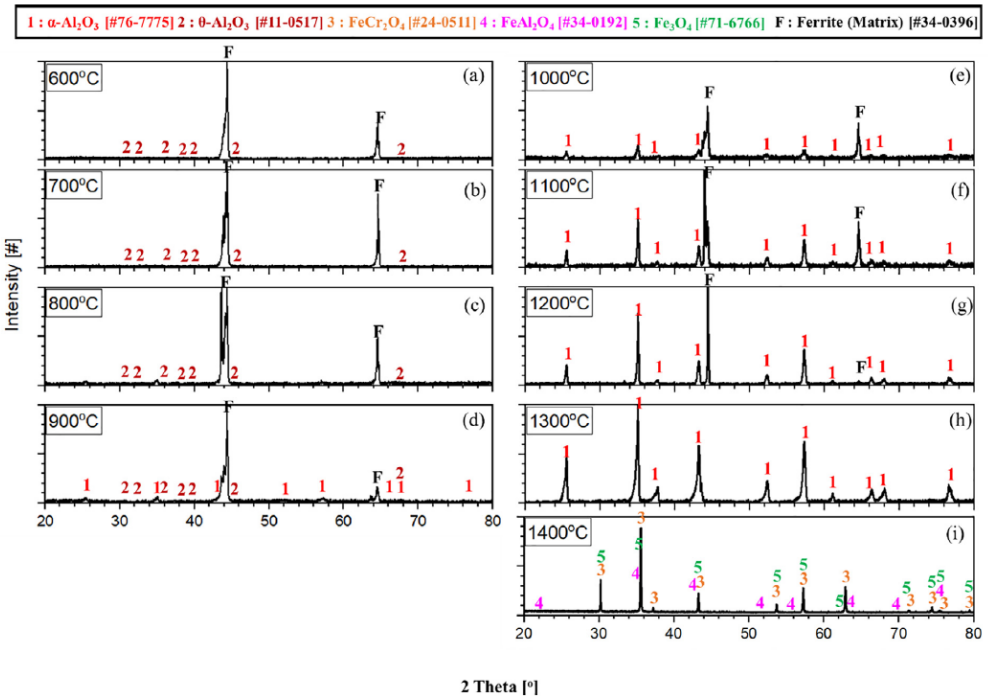

XRD results of the outer surfaces for B136Y3 tube after the isothermal steam oxidation at 600 °C to 1400 °C for 20 h (Kim, 2022)

ATF Characteristics & Experiments

FeCrAl alloys: HT steam oxidation

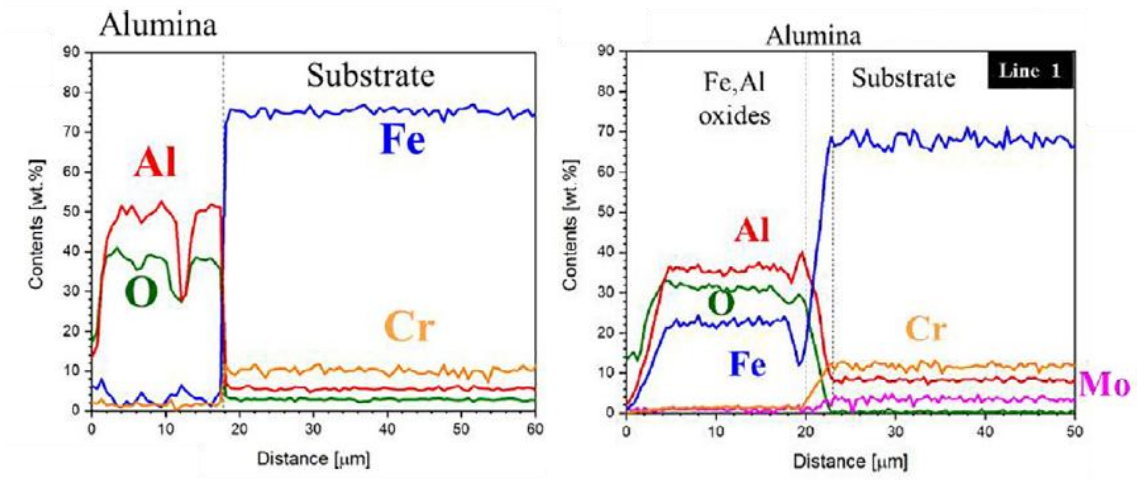

Elements profile along the sample thickness. Left: B136Y3 isothermal test at 1300°C. Right: C26M2 isothermal test at 1500°C. [5]

$$k_p\left[\frac{kg^2}{m^4 s}\right] = \begin{cases} 5.3758 \times 10^{-3} \exp\left(-\frac{184730\ [J/mol]}{RT}\right), & 873\ K < T < 1173\ K \quad (\theta - alumina) \\ 4.69156 \times 10^{-12}, & 1173\ K \leq T \leq 1273\ K \quad (intermediate\ T) \\ 5.0176 \exp\left(-\frac{287748\ [J/mol]}{RT}\right), & 1273\ K < T < 1648\ K\ (\alpha - alumina) \\ 2.4 \times 10^{8} \exp\left(-\frac{352711.2\ [J/mol]}{RT}\right), & T \geq 1648\ K\ (FeO\ melting\ point) \end{cases}$$

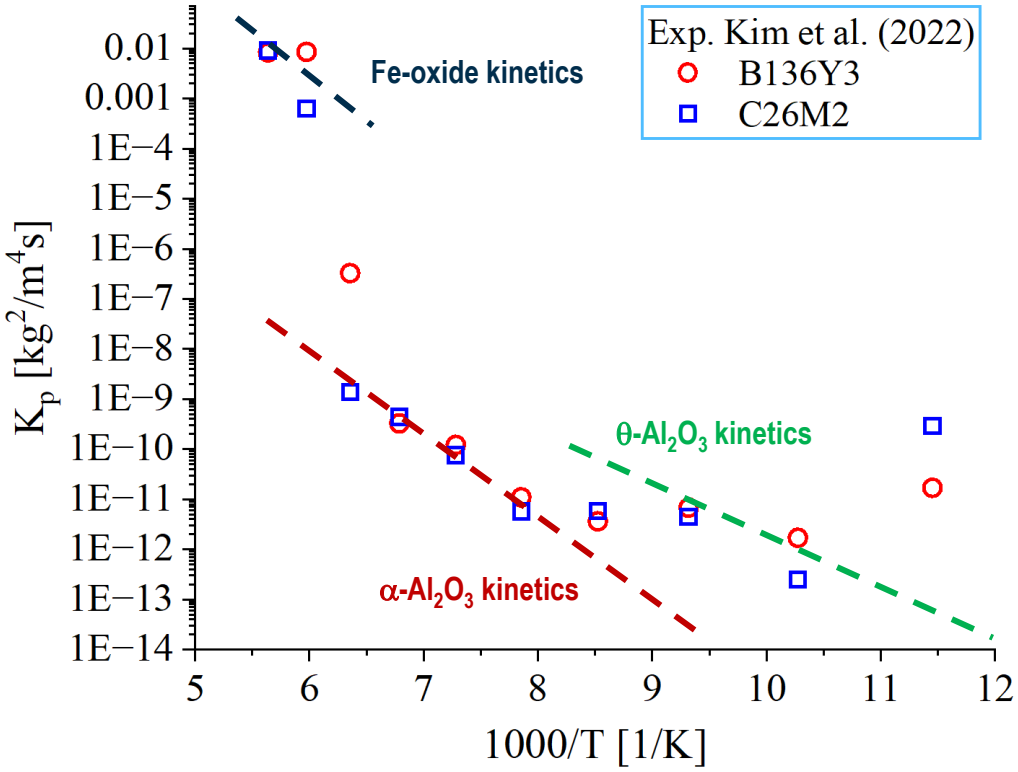

Parabolic rate constants of B136Y3 and C26M2 as a function of temperature with the parabolic constants of Fe-oxide , α-alumina and θ-alumina (Kim, 2022).

ATF Characteristics & Experiments

FeCrAl alloys: Burst behaviour under LOCA

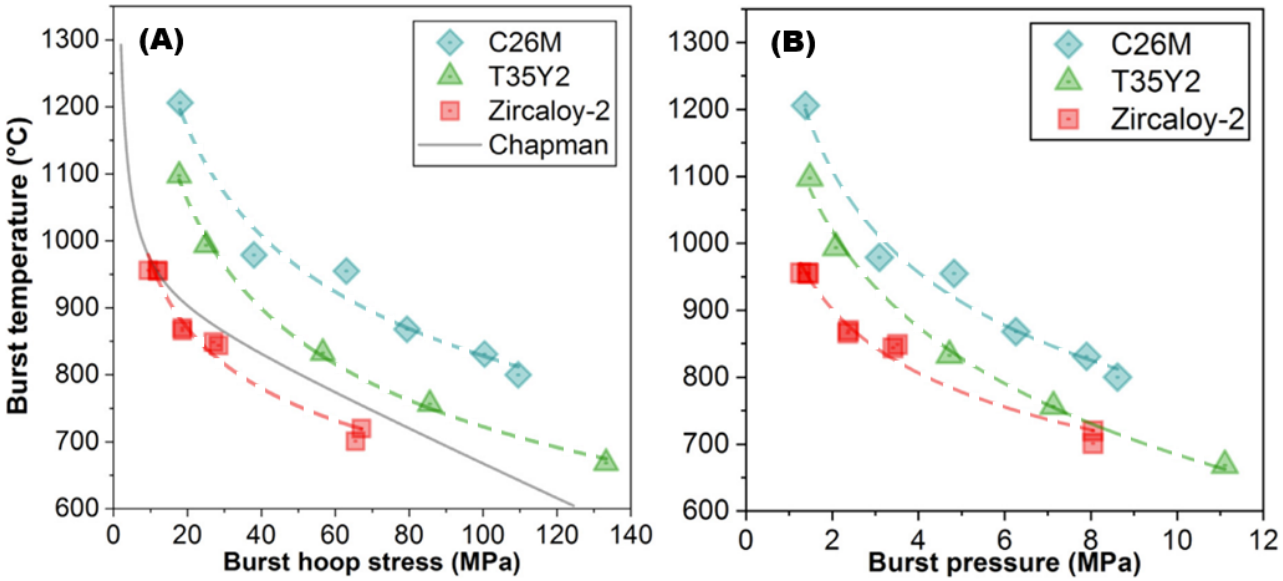

Burst temperature vs (a) engineering hoop stress and (b) rod internal pressure (Bell, 2021).

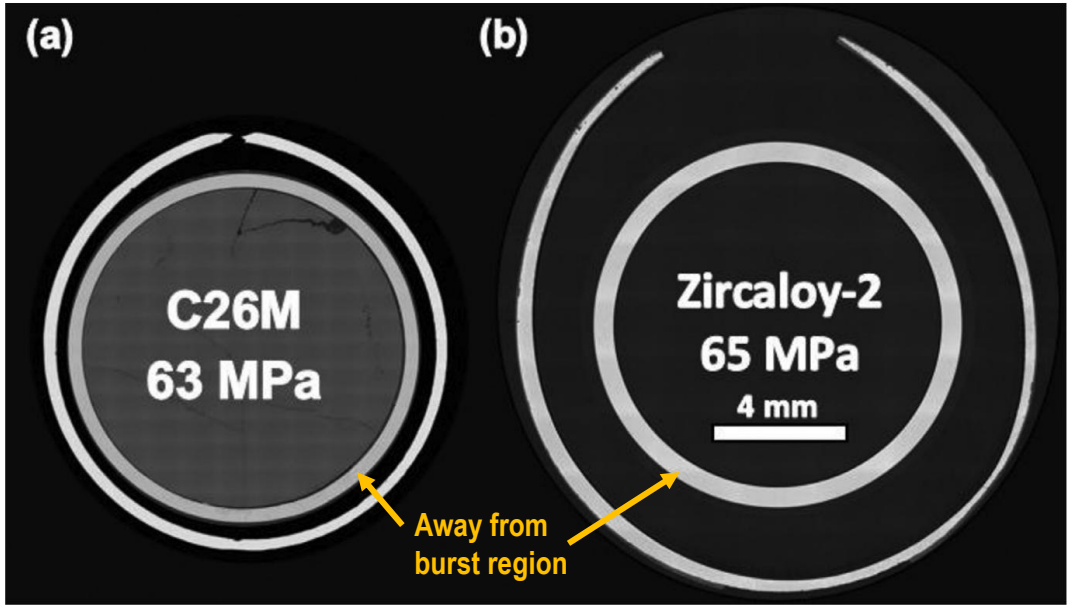

OM for C26M and Zry-2 for samples that burst at ~65 MPa (Bell, 2021).

✓ Higher burst temperature

✓ Lower burst strain

ATF Characteristics & Experiments

Bundle Tests at QUENCH Facility at KIT

OECD/NEA QUENCH-ATF Project (Ongoing)

A unique international experimental program performed at the QUENCH facility (KIT, Germany) to evaluate how ATF claddings behave during LOCA and severe accident conditions.

ATF: Cr-coated Opt. ZIRLO under DBA and BDBA conditions.

QUENCH-19 Experiment

The first integral bundle test worldwide using ATF cladding, performed at the QUENCH facility (KIT, 2018) with FeCrAl alloy (B136Y3) rods.

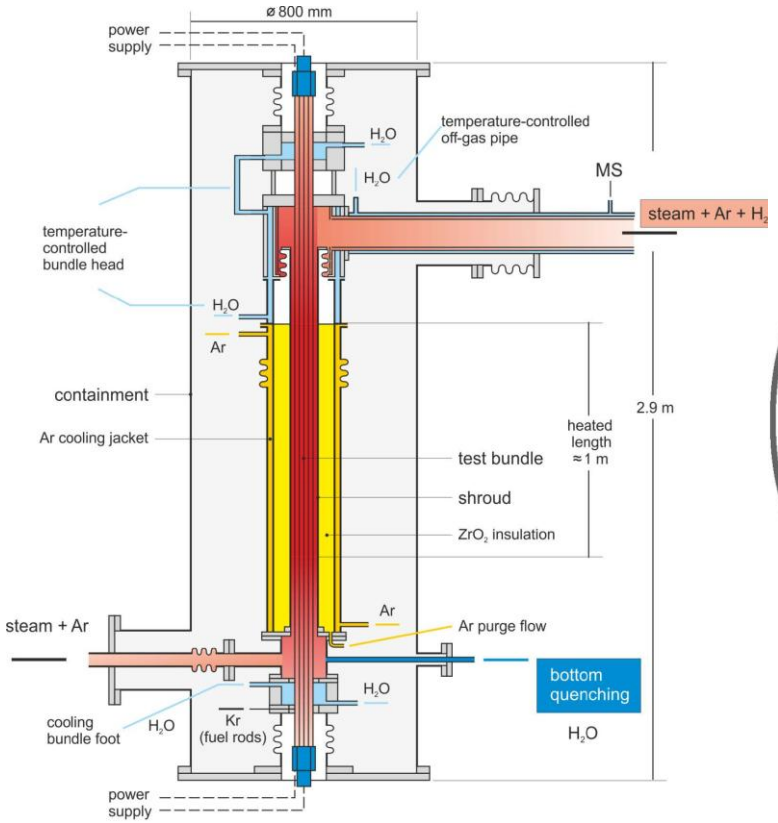

QUENCH-19 Test section (Stuckert, 2022)

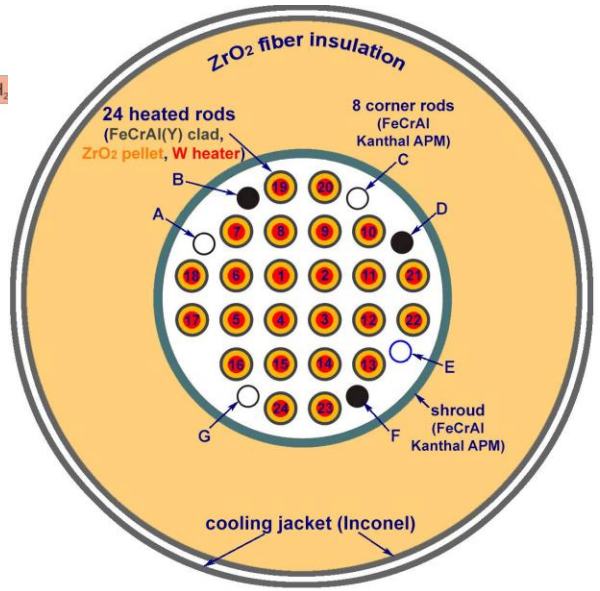

Section of the QUENCH-19 test bundle (Stuckert, 2022)

ATF Characteristics & Experiments

Results QUENCH-19

Main findings

- No temperature runaway during transient when compared to ZIRLO reference, and max. temperatures ~200 K lower in the pre-oxidation phase.
- Large hydrogen reduction: **9.2 g vs 47.6 g (≈-80%).** Lower peak release rate during reflood.
- Oxidation escalation after Al_2O_3 failure (~1650 K).
- Circumferential breaks due to higher thermal expansion of FeCrAl and local melting.

Time (s)	Event
0	Start data recording, el. power 4.86 kW
0...6017	El. power regulated by TFS
6018	Transient stage, el. power rate 5.88 W/s
7127	Switch to constant el. power 18.32 kW
9108..9126	Decrease el. power from 18.32 to 4.34 kW
9110	T_{max} reached: extrapolated TFS1/13 ≈ 1800 K
9114	Switch of carry Ar flow from bundle bottom to top
9116	Start of quench water flow
9119	Massive failure of clads (inner rod P decrease)
9482	Max water level reached = 1319 mm
9760	Quench pump shut off

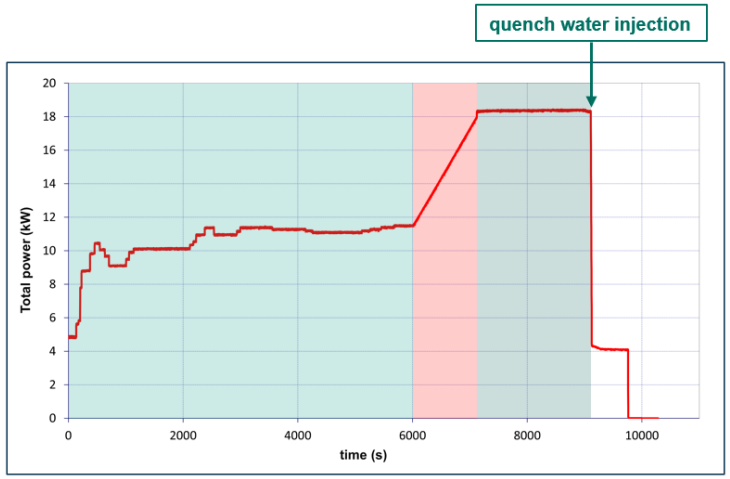

QUENCH-19 Electric power (Rosi, 2026; Stuckert, 2022)

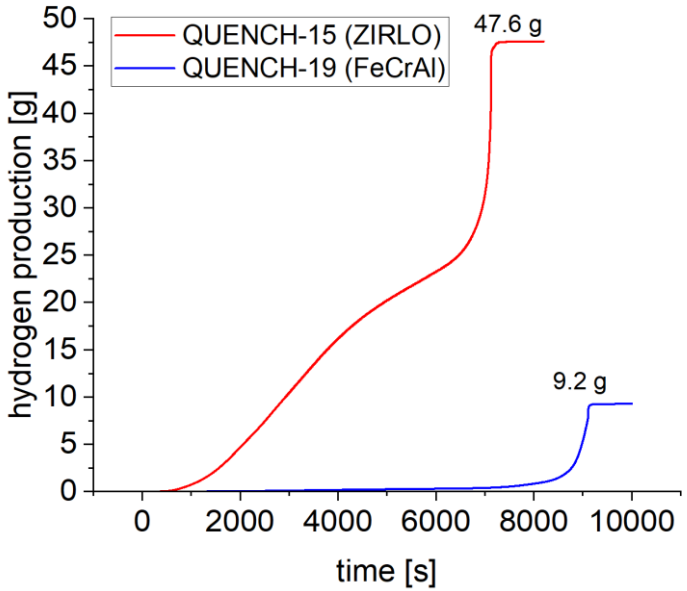

Hydrogen generation comparison between ZIRLO and FeCrAl cladding (Stuckert, 2022)

Computational Modelling Approaches

ASTEC code

- ✓ ASTEC - Accident Source Term Evaluation Code developed by ASNR
- ✓ The code simulate the complete accident sequence in NPPs, from the initial event to the release of radioactive materials

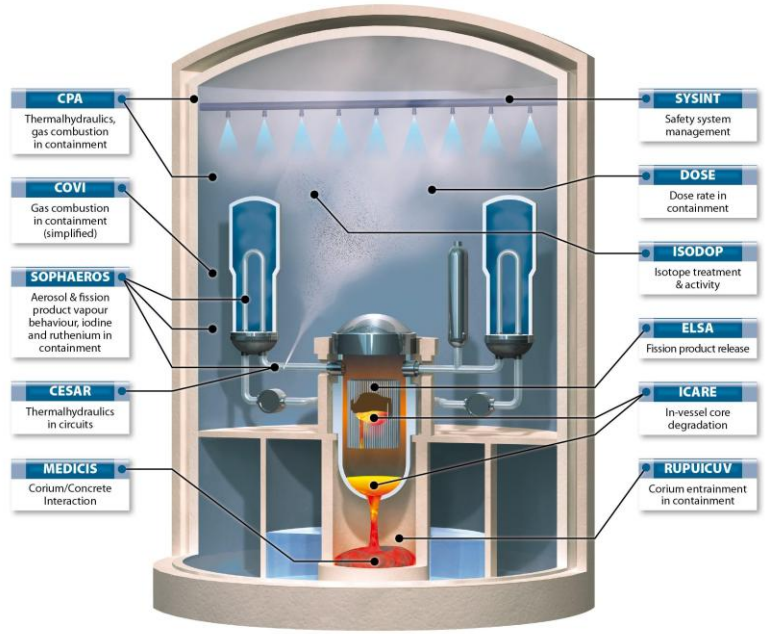

FeCrAl

- No built-in models in the version used
- Currently, under development by KIT with ASNR support.
- Used the Zr-based alloy structure in ASTEC but replaced its in the MDB structure.

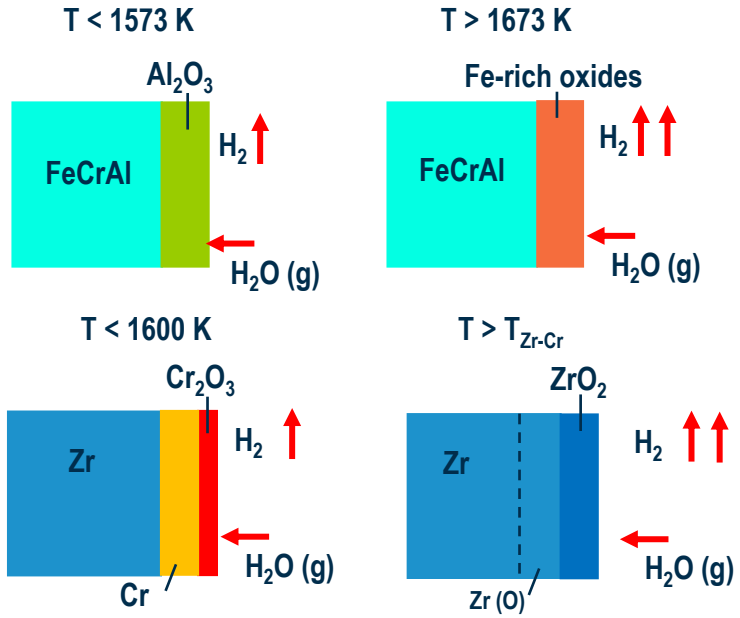

Cr-Coated Zircaloy

- A preliminary modelling approach is being assessed by ASNR.

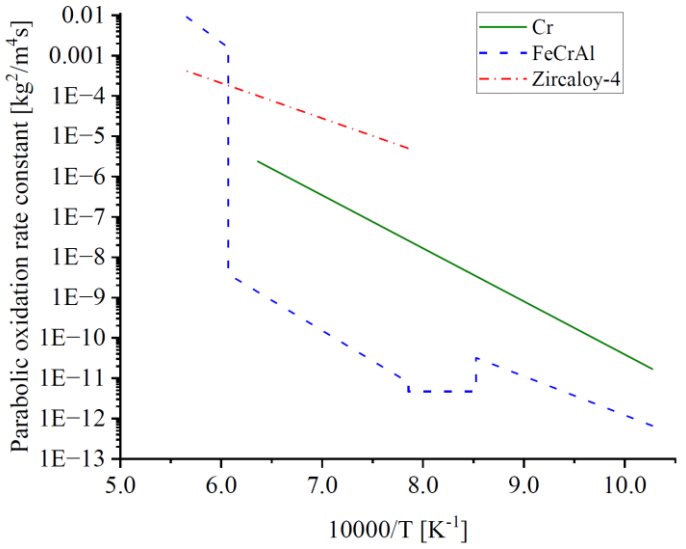

Parabolic law of the oxidation is proven experimentally for both types of ATF material.

- ✓ FeCrAl alloy correlation based on Kim et al. (2022) data
- ✓ Cr-coated Zr-based alloy correlation based on Brachet et al. (2020) data.

(Cazado et al., 2025)

Computational Modelling Approaches

MELCOR Code

- ✓ MELCOR is a fully integrated, engineering-level severe accident simulation code developed by Sandia National Laboratories.
- ✓ It is a system-level tool designed to analyze accident progression.

Main Capabilities

MELCOR provides fully coupled, multi-physics modeling of severe accident phenomena, including:

- Two-phase thermal-hydraulics from the reactor coolant system to containment and ultimately the environment.
- Core heat-up, degradation, and material relocation (both in-vessel and ex-vessel).
- Core-concrete interaction following vessel failure.
- Hydrogen generation, transport, and combustion.
- Fission product release and transport, including vapor and aerosol behavior

Sandia National Laboratories (2026, online)

Computational Modelling Approaches

Modelling QUENCH-19 Bundle Test: ASTEC

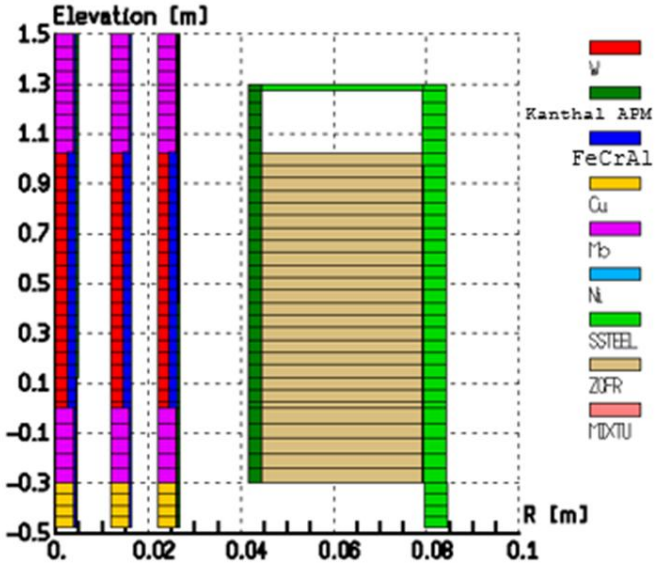

QUENCH Bundle representation with ASTEC (Gabrielli, 2023; Stuckert, 2022)

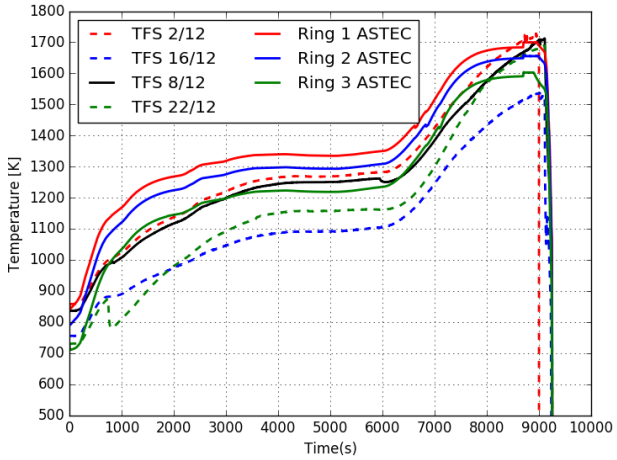

Temperature in different rings: Simulation vs experiment (Gabrielli, 2023; Stuckert, 2022)

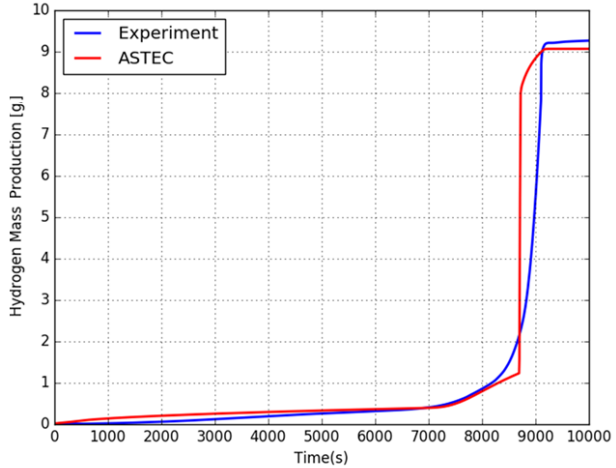

Hydrogen release comparison QUENCH-19 (Gabrielli, 2023; Stuckert, 2022)

- **Maximum temperatures are reasonably well reproduced**
- **The final amount of H_2 is reasonably well reproduced**
- ASTEC results show good agreement with exp. data up about 8000 s
- Escalation is anticipated in time with about 50% of the mass rate compared with the experiment

Computational Modelling Approaches

Modelling QUENCH-19 Bundle Test: MELCOR

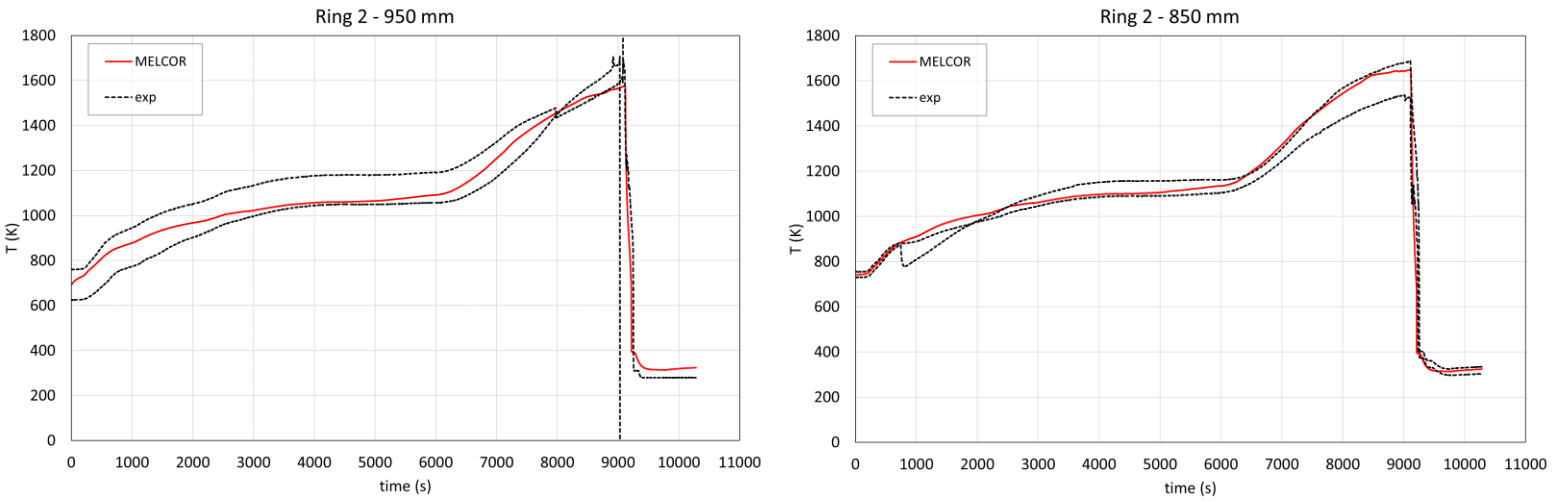

Cladding temperature at 950 mm (left) and 850 mm (right) elevation in Ring 2 (Rosi, 2026; Stuckert, 2022)

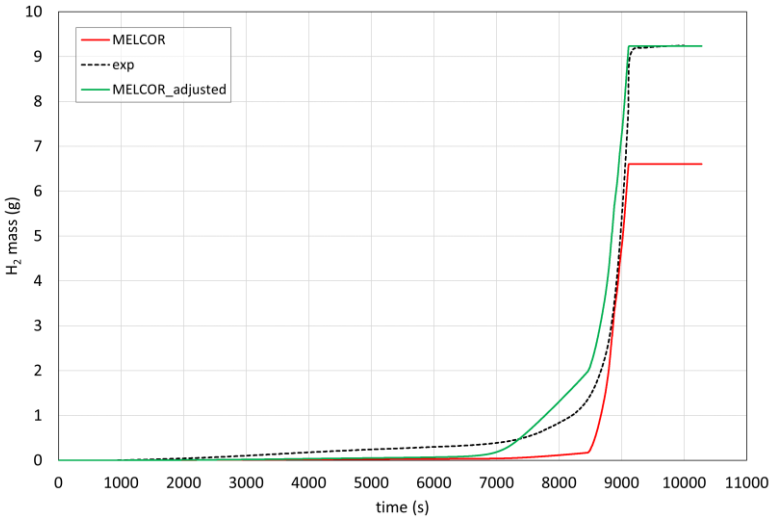

Cumulative Hydrogen production: Simulation vs Exp. (Rosi, 2026; Stuckert, 2022)

- **SS oxidation from the TC sheath have a stronger impact in the bundle experiment with ATF**
- **General good agreement in temperatures and hydrogen generation.**

This work was carried out within the MSc thesis of F. Rosi (University of Pisa) under a mobility grant from the SEAKNOT project.

Computational Modelling Approaches

Generic iPWR Design Assessment with ATF claddings

- Power: 160 MWth
- Natural-circulation pressurized water reactor.
- Integrated reactor: core, pressurizer, helical-tube steam generators (HTSGs), Hot leg riser and Downcomer in RPV.
- RPV surrounded by Steel containment vessel immerse in a water pool.

Safety systems:

- Emergency Core Cooling Systems (ECCS): Primary coolant is collected at the Cont. and recirculation valves opens to generate a flow path.
- Containment Heat Removal System (CHRS): transfer energy to the pool by conduction and convection modes.

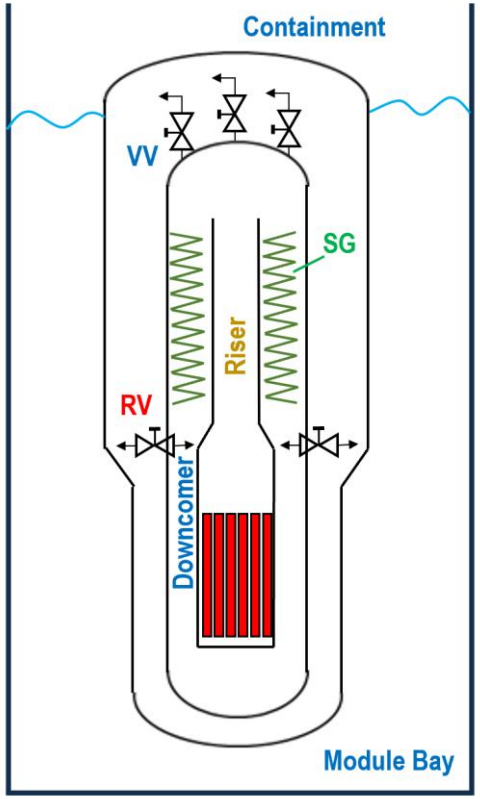

Break on CVCS discharge line 1.69” diameter

Break elevation: 9 [m] from the bottom of cont. to avoid reverse flow.

- Loss AC (Feedwater, CVCS)
- ECCS activation ($DP_{Cont\text{-}RPV}$ < 6.9 MPa & Cont. level > ~5.8 m)
- 3 VVs are available
- 2 RVs fail

Initial conditions

Module water level : 16.8 m
Pool water temperature : 320 K
Initial core power 160 MWt
Decay Heat: EOC – 60 MWd/tU

(Cazado et al., 2025)

Computational Modelling Approaches

Generic iPWR Design Assessment with ATF claddings – Hydrogen release

- The FeCrAl case shows a hydrogen release of approximately 11 kg → **60% reduction compared to Zircaloy-4**. The onset of release is delayed by ~2000 s.
- The Cr-coated Zircaloy case shows a **30% reduction in total hydrogen generation compared to Zircaloy-4**.
- Cladding H_2 generation account for ~44% of total.
- The improved performance of ATFs in the early degradation phase (below ~1600 K) is explained by their superior oxidation resistance.
- Above ~1600-1650 K, the protective effects of both ATFs are lost, and the oxidation rates increase significantly.

Intact rod geom.	H_2 - Zircaloy	H_2 - FeCrAl	H_2 – Cr-coated Zircaloy
~90%	4.2 kg	2.3 kg (-44%)	3.9 kg (-7%)
~50%	21.3 kg	6.4 kg (-70%)	16 kg (-25%)

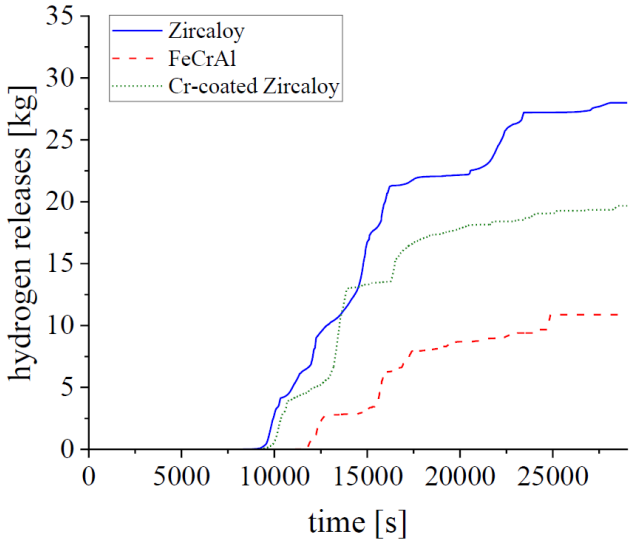

Cumulated hydrogen mass generated only by the cladding oxidation for different materials during the accident sequence.

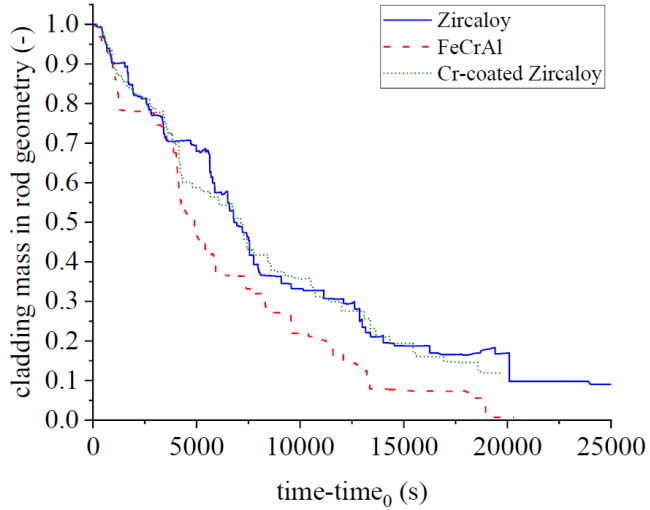

Evolution of the total cladding mass in rod geometry for the different materials used in the simulated sequence.

(Cazado et al., 2025)

Computational Modelling Approaches

Generic BWR Mark-I reactor assessment with ATF: SBO scenario

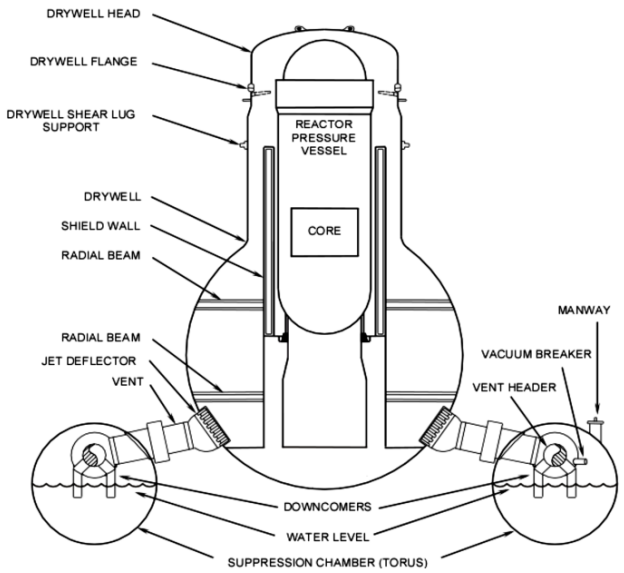

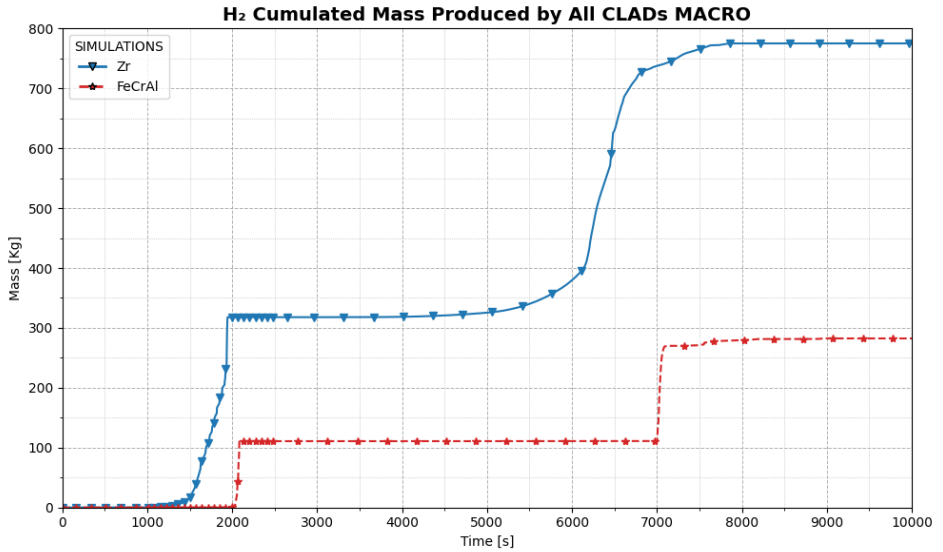

Core:
Thermal Power 4016 MWt -
GE14 10x10 Fuel Assemblies.
Active Core height ~ 3.7 m

The implementation of **ATF cladding** in ASTEC shows:
Delayed cladding failure and temperature escalation
Strong reduction of oxidation
Significant decrease in hydrogen production

This work was carried out within the MSc thesis of E. Gazzola (University of Pisa) under a mobility grant from the SEAKNOT project.

Conclusions

- Advanced Technology Fuels offer is a potential solution in increase the safety margins of current and future light water reactors (LWRs) and small modular reactors (SMRs) without requiring a fundamental change in reactor technology.
- Advanced fuel concepts, such as doped and high-thermal conductivity UO_2, and advanced claddings, such as Cr-coated Zr alloys and FeCrAl, demonstrate measurable improvements in key safety-relevant phenomena:

  Reduced high-temperature steam oxidation rates.
  Significant hydrogen generation mitigation below ~1300°C.
  Potential delayed temperature escalation and extended coping time.

- Separate Effect Tests and Bundle experiments provide strong evidence of oxidation resistance.
- There are still challanges to be addressed: Eutectic interactions, hydrogen permeability, extense irradiation behaviour, etc.

Conclusions

- Current Systems codes like ASTEC and MELCOR are able to reproduce adequately the oxidation behaviour of ATF claddings under high temperature steam.
- During the reactor simulations (iPWR & BWR) under SA conditions, ATF cladding materials have a clear and positive impact on core heating and hydrogen production during the early phases of hypothetical sequence.
- The superior oxidation resistance of FeCrAl and Cr-coated Zircaloy at temperatures below ~1600 K is the main reason for these benefits.
- Although significant progress has been made in modelling ATF behaviour, further development and validation of models for late in-vessel degradation are still required, particularly regarding interaction with UO_2 and melt formation, to improve safety assessments and predictive capability.

References

- Arias, D., Abriata, J. P. (1986). The Cr–Zr (chromium–zirconium) system. *Bulletin of Alloy Phase Diagrams*, 7(3).
- Aragon, P., et al. (2022). Modelling FeCrAl cladding thermo-mechanical performance. Part I: Steady-state conditions. *Progress in Nuclear Energy*, 153.
- Bell, S. B., et al. (2021). Strength and rupture geometry of un-irradiated C26M FeCrAl under LOCA burst testing conditions. *Journal of Nuclear Materials*, 557.
- Bischoff, J., et al. (2016). Development of Cr-coated zirconium alloy cladding for enhanced accident tolerance. *TopFuel 2016 – Light Water Reactor (LWR) Fuel Performance Meeting*, Boise, USA.
- Bourgeois, L., et al. (2001). Factors governing microstructure development of Cr_2O_3-doped UO_2 during sintering. *Journal of Nuclear Materials,* 297(3).
- Brachet, J. C., et al. (2016). Behavior under LOCA conditions of enhanced accident-tolerant chromium-coated Zircaloy-4 claddings. *TopFuel 2016 – Light Water Reactor (LWR) Fuel Performance Meeting*, Boise, USA.
- Brachet, J. C., et al. (2020). High temperature steam oxidation of chromium-coated zirconium-based alloys: Kinetics and process. *Corrosion Science*, 167.
- Cazado, M. E., et al. (2025). Impact of advanced technology fuel cladding materials on the progression of severe accidents in a generic natural-circulation iPWR. *NURETH-21*, Busan, Korea.
- Delafoy, D., Arimescu, I. (2016). Developments in fuel design and manufacturing to enhance PCI performance of AREVA NP fuel. *Workshop Proceedings NEA Working Group on Fuel Safety*, Lucca, Italy.
- Deng, J., et al. (2023). Steam oxidation of Cr-coated zirconium alloy claddings at 1200 °C: Kinetics transition and failure mechanism of Cr coatings. *Journal of Nuclear Materials 586*.
- Fairewinds Energy Education (2026). Japan's Fukushima meltdowns — 10 years later: New video shows much still unknown. Available online. https://www.fairewinds.org/demystify/japans-fukushima-meltdowns-10-years-later-new-video-shows-much-still-unknown
- Gabrielli, F., et al. (2023). KIT validation activities of the ASTEC code against the QUENCH bundle experiments: Results and outlook. *28th International QUENCH Workshop*, Karlsruhe, Germany.
- Gazzola, E., et al. (2026). Accepted contribution Poster. Impact of FeCrAl Cladding Material on the Progression of a Severe Accident in a Generic BWR Mark-I NPP: analysis of a SBO Scenario with the ASTEC Code. *ERMSAR 2026*.
- Hu, X., et al. (2015). Hydrogen permeation in FeCrAl alloys for LWR cladding application. *Journal of Nuclear Materials*, 461.
- IAEA (2018). State-of-the-art report on light water reactor accident-tolerant fuels. *International Atomic Energy Agency*.

References

- Kim, D. J., et al. (2018). Development status of microcell UO_2 pellet for accident-tolerant fuel. *Nuclear Engineering and Technology*, 50.
- Kim, D. J., et al. (2023). Development status of high thermal conductive ATF pellet and burnable absorber fuel pellet. *IAEA Technical Meeting on Advances in Nuclear Fuel Fabrication Technologies*, Vienna, Austria.
- Kim, H. G., et al. (2016). Development status of accident-tolerant fuel for light water reactors in Korea. *Nuclear Engineering and Technology*, 48(1).
- Kim, C., et al. (2022). Oxidation mechanisms and kinetics of nuclear-grade FeCrAl alloy in the temperature range of 500–1500 °C in steam. *Journal of Nuclear Materials*, 564.
- Koyanagi, T., et al. (2017). SiC/SiC cladding materials properties handbook. ORNL/SPR-2017/385.
- Massey, C. P., et al. (2016). Cladding burst behavior of Fe-based alloy under LOCA. *Journal of Nuclear Materials*, 470.
- Ott, L. J., Robb, K. R., Wang, D. (2014). Preliminary assessment of accident-tolerant fuels on LWR performance during normal operation and DB and BDB accident conditions. *Journal of Nuclear Materials*, 448.
- Rosi, F., et al. (2026). Accepted contribution Poster. Assessing the capabilities of MELCOR V2.2 against the QUENCH-19 Bundle Test with FeCrAl Cladding. *ERMSAR 2026*.
- Sandia National Laboratories. MELCOR: Light and Non-Light Reactor Applications. Available Online: https://www.sandia.gov/MELCOR/light-and-non-light-water-reactor-applications/
- Schuster, F., et al. (2015). On-going studies at CEA on chromium-coated zirconium-based nuclear fuel claddings for enhanced accident-tolerant LWR fuel. *TopFuel 2015 - Reactor Fuel Performance Meeting*, Zurich, Switzerland.
- Steinbrück, M., et al. (2024). Overview of mechanisms of degradation of promising ATF cladding materials during oxidation at high temperatures. *High Temperature Corrosion of Materials*, 101.
- Stuckert, J., et al. (2022). Results of the bundle test QUENCH-19 with FeCrAl claddings. KIT Scientific Report NUSAFE-3575.
- Terrani, K. A. (2018). Accident tolerant fuel cladding development: Promise, status, and challenges. *Journal of Nuclear Materials*, 501.